

Genetic and Physiological Diversity in the Leaf Photosynthetic Capacity of Soybean

Kazuma Sakoda, Yu Tanaka,* Stephen P. Long, and Tatsuhiko Shiraiwa

ABSTRACT

Enhancement of leaf photosynthetic capacity can lead to greater biomass productivity in crop plants. Targets for improving leaf photosynthetic capacity in soybean [*Glycine max* (L.) Merr.], however, remain to be elucidated. The objective of this study was to identify the physiological and morphological factors underlying the diverse photosynthetic capacities of different soybean genotypes. Light-saturated CO₂ assimilation rates ranged from 18.1 to 27.6 $\mu\text{mol m}^{-2} \text{s}^{-1}$ under controlled conditions among 34 genotypes. PI 594409 A (Line no. 13) and PI 603911 C (Line no. 14) showed extremely high photosynthetic rates. Line no. 14 consistently showed greater photosynthetic rates than other lines under field conditions and reached 34.8 $\mu\text{mol m}^{-2} \text{s}^{-1}$, which was 11% greater than that of a reference genotype, Tachinagaha. The analysis of the CO₂ response curve of Line no. 14 showed greater CO₂ fixation activity, represented by the maximum rates of carboxylation ($V_{c_{\max}}$) and electron transport (J_{\max}). The leaf ribulose-1,5-bisphosphate carboxylase/oxygenase (Rubisco) content of Line no. 14 tended to be higher than that of other lines, which is suggested to contribute to high CO₂ fixation activity. We attribute the high photosynthetic capacity that was observed among soybean genotypes to high CO₂ fixation activity.

K. Sakoda, Y. Tanaka, and T. Shiraiwa, Graduate School of Agriculture, Kyoto Univ., Kitashirakawa Oiwake-cho, Sakyo-ku, Kyoto 606-8502, Japan; S.P. Long, Dep. of Plant Biology and Institute for Genomic Biology, Univ. of Illinois, Urbana-Champaign, 1206 West Gregory Drive, Urbana, IL 61801, USA. K. Sakoda and Y. Tanaka contributed equally to this work. Received 24 Feb. 2016. Accepted 11 June 2016. *Corresponding author (tanaka12@kais.kyoto-u.ac.jp). Assigned to Associate Editor Thomas Clemente.

Abbreviations: *A*, CO₂ assimilation rate; *C_i*, intercellular CO₂ concentration; DAP, days after planting; *J_{max}*, electron transport; LNC, Leaf N content; PPF, photosynthetic photon flux density; *V_{c_{max}}*, maximum rate of carboxylation.

INCREASES in food production are needed to meet the demand of the rapidly growing human population (Cohen, 2003). Soybean is one of the world's most important crops, and its production is the fourth largest after maize (*Zea mays* L.), rice (*Oryza sativa* L.), and wheat (*Triticum aestivum* L.). Soybean is the main source of protein and oil for humans and livestock (USDA, 2012). There have therefore been numerous attempts to improve soybean seed yield around the world.

It has been reported that improvements in leaf photosynthetic capacity, defined as the photosynthetic rate per unit of leaf area under light-saturated conditions, can contribute to increased primary production and crop yield (Long et al., 2006; Zhu et al., 2010). In previous studies, elevated CO₂ was found to enhance the leaf photosynthetic rate and the seed yield in C3 crops, including soybean (Mitchell et al., 1999; Ainsworth and Long, 2005). It has also been reported that improvements in energy conversion efficiency, mainly determined by the sum of the leaf photosynthesis in the canopy, have been among the major factors historically in increasing biomass productivity in soybean (Koester et al., 2014).

Published in Crop Sci. 56:2731–2741 (2016).
doi: 10.2135/cropsci2016.02.0122

© Crop Science Society of America | 5585 Guilford Rd., Madison, WI 53711 USA
All rights reserved.

These results imply that leaf photosynthetic capacity can be a key trait for increasing the productivity of soybean.

There is natural variation in leaf photosynthetic capacity within a single C3 crop species. Although this variation has often been overlooked, there is great potential for improving leaf photosynthetic capacity by detecting the mechanism that underlies it (Raines, 2011). This natural variation in leaf photosynthetic capacity is caused by physiological and morphological properties that are regulated by environmental and genetic factors (Flood et al., 2011). ‘Takanari’, the high-yielding rice cultivar, shows great leaf photosynthetic capacity (Kanemura et al., 2007). *NAL1*, the first gene that accounts for the natural variation in leaf photosynthesis in rice, was identified by QTL analysis with map-based cloning using Takanari (Takai et al., 2013). Two rice lines with extremely high photosynthetic capacity were selected from among backcrossed inbred lines derived from Takanari and ‘Koshihikari’, a Japanese elite cultivar (Adachi et al., 2013). The high photosynthetic capacity of these lines was attributed to greater mesophyll conductance because of the higher density and better developed lobes of the mesophyll cells. There have been few studies, however, that identify the dominant factors responsible for high photosynthetic capacity in soybean.

Leaf photosynthetic capacity is determined by the CO₂ supply from the atmosphere to the chloroplast and by CO₂ fixation in the chloroplast. Stomatal conductance, which represents the efficiency of the CO₂ supply via the stomata, is regulated by stomatal movement (Lawson and Blatt, 2014). It is also affected by morphological traits such as stomatal density and size (Franks and Beerling, 2009). Leaf N content (LNC) is often correlated with leaf photosynthetic capacity within plant species (Evans, 1989; Hikosaka, 2004). This is because a large amount of leaf N is allocated to the photosynthetic apparatus, especially to ribulose-1,5-bisphosphate carboxylase/oxygenase (Rubisco). In previous studies, a significant correlation between LNC and leaf photosynthetic capacity was observed under different N application regimes in soybean, rice, and maize (Sinclair and Horie, 1989). However, the genetic basis of the relationship between these traits remains to be elucidated under controlled conditions in soybean.

To cover the genetic diversity in the leaf photosynthetic capacity of soybeans, 216 genotypes were randomly selected from the population developed by Ray et al. (2015). Most of the population was occupied by the Asian local varieties. We conducted the preliminary selection based on the leaf temperature measurements as described by Tanaka et al. (2013) to establish a subcollection for the present study. This collection contains 34 genotypes and consists of 16 genotypes with high leaf temperature, 16 genotypes with low temperature, and two commercial varieties. The collection was expected to cover the large diversity of the leaf photosynthetic capacity among soybeans.

In the present study, an initial screening based on photosynthetic rate was conducted under controlled conditions among 34 soybean genotypes, and two unique genotypes were selected for their extremely high photosynthetic rate. Further physiological and morphological analyses were conducted with these genotypes and two commercial cultivars. Through these analyses, we aimed to evaluate the genetic diversity of photosynthetic capacity in soybean and to clarify its physiological and morphological basis to improve future soybean breeding.

MATERIALS AND METHODS

Materials and Cultivation of Plants

We conducted two principal experiments. In Exp. 1, 34 soybean genotypes were sown in 3-L pots containing potting soil (Sunshine Mix #1 LC1, SunGro Horticulture) with a top dressing of Osmocote (Scotts Miracle-Gro). It was reported that the typical Japanese cultivar Tachinagaha (Tc) showed lower photosynthetic capacity than the US cultivar, Stressland (Tanaka et al., 2008). The US commercial cultivar, UA4805 (UA) had higher biomass productivity than Japanese cultivars (Kawasaki et al., 2016). UA4805 also showed the higher stomatal conductance, which could cause high photosynthetic capacity (Tanaka et al., 2010). Based on these previous studies, Tc and UA were used as reference cultivars in all the experiments in the present study. The 34 soybean genotypes belong to maturity group four to five and have a determinate stem growth habit (Table 1). Five pots were prepared per each genotype and each of pot had one plant. The plants were placed randomly and grown in a growth chamber (Conviron, Winnipeg, Manitoba, Canada) with the day–night temperature set to 26 and 20°C and a photoperiod of 14 h. The light intensity was set to a photosynthetic photon flux density (PPFD) of 1200 μmol m⁻² s⁻¹. Plants were watered as needed.

In Exp. 2, PI 594409 A (Line no. 13) and PI 603911 C (Line no. 14) were planted with the Japanese commercial cultivar Tachinagaha (Tc) and the US commercial cultivar UA4805 (UA) at the Experimental Farm of the Graduate School of Agriculture, Kyoto University, Kyoto, Japan (35°2′ N, 135°47′ E, 65 m asl; Fluvic Endoaquepts soil type). Cultivars Tc and UA were used as reference cultivars in both experiments. The sowing date was 25 June 2014. The row and plant spacing distances were 0.7 and 0.2 m, respectively. Nitrogen, P₂O₅, and K₂O fertilizers were applied at 3, 10, and 10 g m⁻², respectively, before sowing. Two replicates of the experimental plot were established for each genotype in a randomized complete block design. Each experimental plot was composed of 33 plants in three rows and each row had 11 plants. The date was recorded when the plants reached to the beginning of the flowering (R1) and to the beginning of the seed filling (R5).

Gas Exchange Measurement

Leaf gas exchange was measured with a portable gas-exchange system (LI-6400, LI-COR). In Exp. 1, the CO₂ assimilation rate (A_{380}) and the stomatal conductance were measured at a CO₂ concentration of 380 μmol mol⁻¹, a PPFD of 2000 μmol m⁻² s⁻¹, and an air temperature of 26°C from the youngest fully expanded leaf at 26 d after planting (DAP). The plants were at the fourth trifoliate stage.

Table 1. List of line number, plant introduction (PI) number, the stem growth habit, and maturity group of 34 soybean genotypes.

PI no.	Line no.	Growth habit	Maturity group
PI 360848	15	D-type	4
PI 398200	16	D-type	4
PI 398334	17	D-type	4
PI 398406	18	D-type	4
PI 398695	19	D-type	4
PI 398915	20	D-type	4
PI 399027	1	D-type	4
PI 399094	2	D-type	4
PI 404159	21	D-type	4
PI 407832 B	22	D-type	4
PI 407959 A	3	D-type	4
PI 408073	23	D-type	4
PI 408111	24	D-type	4
PI 408131 B	25	D-type	4
PI 408140 B	4	D-type	4
PI 408269 A	5	D-type	4
PI 417107	6	D-type	4
PI 417345 A	26	D-type	4
PI 423888	7	D-type	4
PI 424149	27	D-type	4
PI 424296 A	28	D-type	4
PI 424381	8	D-type	4
PI 424402 A	9	D-type	4
PI 424489 B	10	D-type	4
PI 424511	29	D-type	4
PI 424549 A	11	D-type	4
PI 442012 B	30	D-type	4
PI 458098	31	D-type	4
PI 592940	12	D-type	4
PI 594287	Tc	D-type	Not available
PI 639187	UA	D-type	4.8
PI 567174 C	32	D-type	4
PI 594409 A	13	D-type	4
PI 603911 C	14	D-type	4

In Exp. 2, the CO₂ assimilation rate (A_{400}) and the stomatal conductance were measured in the field at a CO₂ concentration of 400 $\mu\text{mol mol}^{-1}$, a PPFD of 2000 $\mu\text{mol m}^{-2} \text{s}^{-1}$, and an air temperature of 33°C from the upper-most fully expanded leaf at 33, 57, 65, and 72 DAP (from R1 to R5). The CO₂ assimilation rate (A) at several intercellular CO₂ concentrations (C_i) was also measured at the upper-most fully expanded leaf at 57, 69, and 71 DAP. The CO₂ concentration in the chamber was set to 100, 200, 300, 400, 500, 600, 750, and 1000 $\mu\text{mol mol}^{-1}$. The light intensity was a PPFD of 2000 $\mu\text{mol m}^{-2} \text{s}^{-1}$ and the air temperature was 33°C in the chamber. The $A-C_i$ curves were analyzed to estimate $V_{c_{\max}}$ and J_{\max} , defined as the maximum rates of carboxylation and electron transport, respectively, using the biochemical model described by Farquhar et al. (1980) with modifications by Bernacchi et al. (2001) and McMurtrie and Wang (1993) (Eqn. [1] and [2]):

$$A = \frac{V_{c_{\max}}(C_i - \Gamma^*)}{C_i + K_c \left(1 + \frac{O}{K_o}\right)} - R_m \quad [1]$$

$$A = \frac{J_{\max}(C_i - \Gamma^*)}{4C_i + 8\Gamma^*} - R_m \quad [2]$$

where Γ^* is the CO₂ photocompensation point, R_m is the rate of daytime mitochondrial respiration, and K_c and K_o is Michaelis-Menten constant of Rubisco for CO₂ and O₂, respectively. The values of these parameters were applied from Bernacchi et al. (2001).

Quantification of Leaf Components

The total soluble protein, chlorophyll, Rubisco, and N contents were determined at the same leaf position as the leaf gas exchange measurement used in Exp. 2. A leaf tissue area of 4.52 cm² was collected from the leaf and the area of the remainder was measured. The remainder was dried at 60°C for 72 h, weighed, and ground for the measurement of LNC. The LNC was determined by Kjeldahl digestion followed by an indophenol assay. Leaf tissues were homogenized using a cold mortar and pestle in the extraction buffer, containing 50 mM HEPES-KOH, 5 mM MgCl₂, 1 mM EDTA, 0.1% (w/v) PVPP, 0.05% (v/v) Triton X-100, 5% glycerol, 4 mM amino-n-caproic acid, 0.8 mM benzamidine-HCl, and 5 mM DTT at pH 7.4 with a small amount of quartz sand. A 200- μL aliquot was set aside for the chlorophyll quantification. The homogenate was centrifuged at 14,500 g for 5 min at 4°C. The supernatant was used for the quantification of total soluble protein and Rubisco with bovine serum albumin as the standard. The total soluble protein content was determined by the Bradford assay (Bradford, 1976). The Rubisco content was quantified as described by Makino et al. (1986). The chlorophyll content was determined spectrophotometrically as described by Porra et al. (1989).

Leaf Anatomy

In Exp. 2, the leaf anatomical structure was analyzed in a resin section prepared as follows. Leaf samples (5 by 5 mm) were collected from the leaf from which the $A-C_i$ curves were obtained on 67 and 71 DAP. They were fixed in FAA solution (ethanol/water/formalin/acetic acid, 12:6:1:1 v/v). Subsequently, the leaf tissues were dehydrated in a graduated ethanol series and the ethanol inside the leaf tissues was replaced by Technobit 7100 resin (Heraeus Kulzer). The solidified resin including the leaf tissue was prepared following the manufacturer's protocol and cut into 5 μm sections using a motorized rotary microtome (RM2155, Leica). The sections were colored with 0.05% toluidine blue solution for 30 min and rinsed with water for 5 min. Microscopic images were obtained with an optical microscope (Olympus CX31 and Olympus DP21, Olympus). The leaf thickness and the palisade layer thickness were measured using the image analysis software ImageJ (Schneider et al., 2012).

Statistical Analysis

In Exp. 1, the variation of leaf gas exchange capacity among 34 genotypes was evaluated by Tukey's multiple comparison.

Table 2. Phenology of the materials.

PI no.	Line no.	Days after planting	
		R1†	R5‡
PI 594287	Tc	33	54
PI 594409 A	13	40	63
PI 603911 C	14	33	54
PI 639187	UA	42	63

† R1, beginning of the flowering.

‡ R5, beginning of the seed filling.

In Exp. 2, one-way ANOVA was applied for statistical analysis of leaf gas exchange capacity. The variation of the leaf morphological property among four genotypes was evaluated by Tukey's multiple comparison in Exp. 2. All analyses were conducted using R (R Development Core Team, 2010).

RESULTS

Phenology of the Materials

In Exp. 2, Line no. 14, Tc, Line no. 13, and UA reached to R1 at 33, 33, 40, and 42 DAP, respectively (Table 2). Line no. 14, Tc, Line no. 13, and UA reached to R5 at 54, 54, 63, and 63 DAP, respectively.

Leaf Gas Exchange Capacity

In Exp. 1, leaf photosynthetic capacity was analyzed in the 34 genotypes at the fourth trifoliolate stage under controlled conditions. The A_{380} value ranged from 18.1 $\mu\text{mol m}^{-2} \text{s}^{-1}$ in Line no. 18 to 28.7 $\mu\text{mol m}^{-2} \text{s}^{-1}$ in Line no. 13 (Fig. 1A). The A_{380} value of Line no. 14 was 27.2 $\mu\text{mol m}^{-2} \text{s}^{-1}$, and it was the second highest among all the genotypes. There was the significant difference of A_{380} between Line no. 13 against Lines no. 1, 2, 11, 18, 19, 21, and 22 ($P < 0.05$). The significant difference was also observed between Line no. 14 against Lines no. 18 and 22. The A_{380} values of Lines no. 13 and 14 were more than 10% greater than the two reference cultivars, Tc and UA. Stomatal conductance varied from 0.43 $\text{mol m}^{-2} \text{s}^{-1}$ in Line no. 8 to 0.80 $\text{mol m}^{-2} \text{s}^{-1}$ in Line no. 24 but there was no significant difference of the stomatal conductance among all the genotypes (Fig. 1B). The stomatal conductance of Line no. 13 was the second highest among all the genotypes, while that of Line no. 14 was intermediate.

In Exp. 2, leaf photosynthetic capacity was measured in four genotypes from the flowering to the seed filling stage under field conditions. The A_{400} value was stable within each of four genotypes from 33 to 65 DAP, but it drastically decreased at 72 DAP (Fig. 2A). The A_{400} value of Line no. 14 was consistently higher than that of the others in all measurements. At 65 DAP, the A_{400} of Line no. 14 was 34.8 $\mu\text{mol m}^{-2} \text{s}^{-1}$, which was 11% higher than that of the reference cultivar Tc. The A_{400} value of Line no. 13 was similar to that of UA. However, there was no clear trend in the variation in stomatal conductance among the four genotypes (Fig. 2B). The value of A_{400} divided by C_i

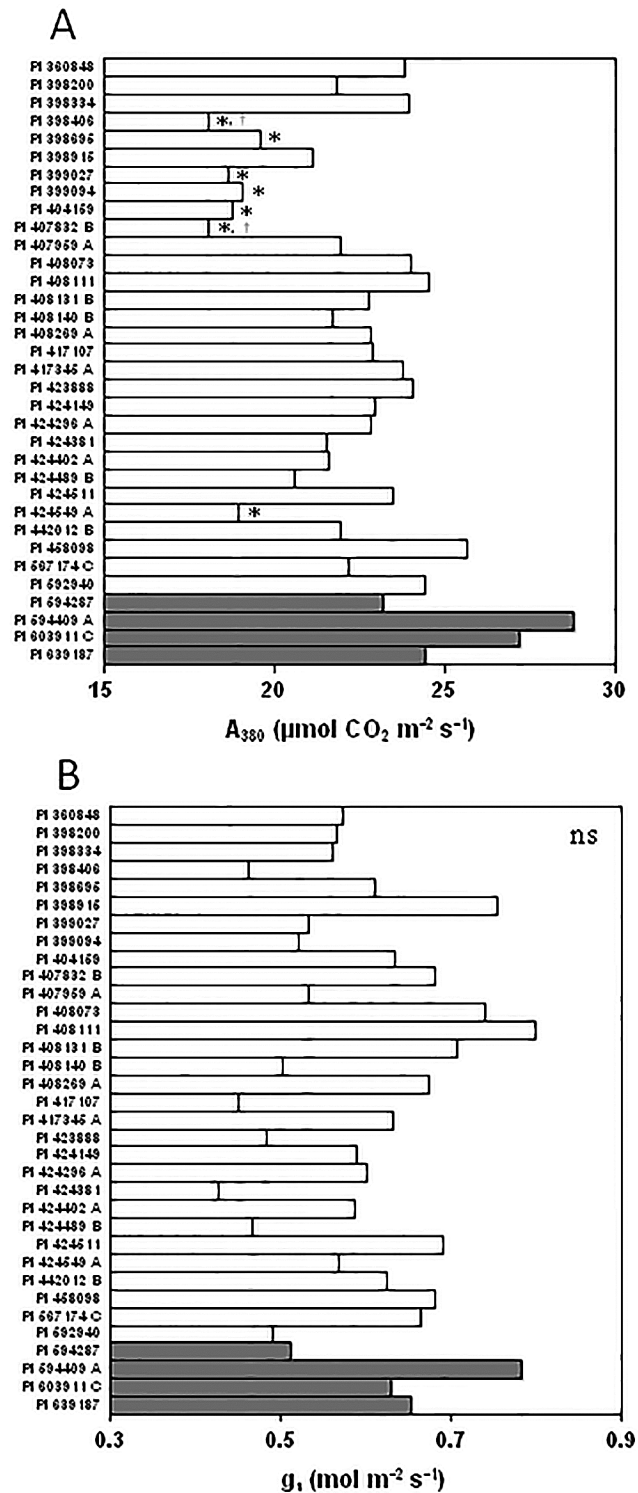


Fig. 1. CO₂ assimilation rate and stomatal conductance among 34 soybean genotypes. The CO₂ assimilation rate (A_{380}) and the stomatal conductance at a CO₂ concentration of 380 $\mu\text{mol mol}^{-1}$ were measured under controlled conditions at 26 d after planting (the fourth trifoliolate stage) in 34 soybean genotypes. The asterisk (*) and dagger (†) symbols following each bar indicates the significant difference at $P < 0.05$ against PI 594409 A (Line no. 13) and PI 603911 C (Line no. 14), respectively. The letters ns indicate no significant difference at $P < 0.05$ among 34 soybean genotypes.

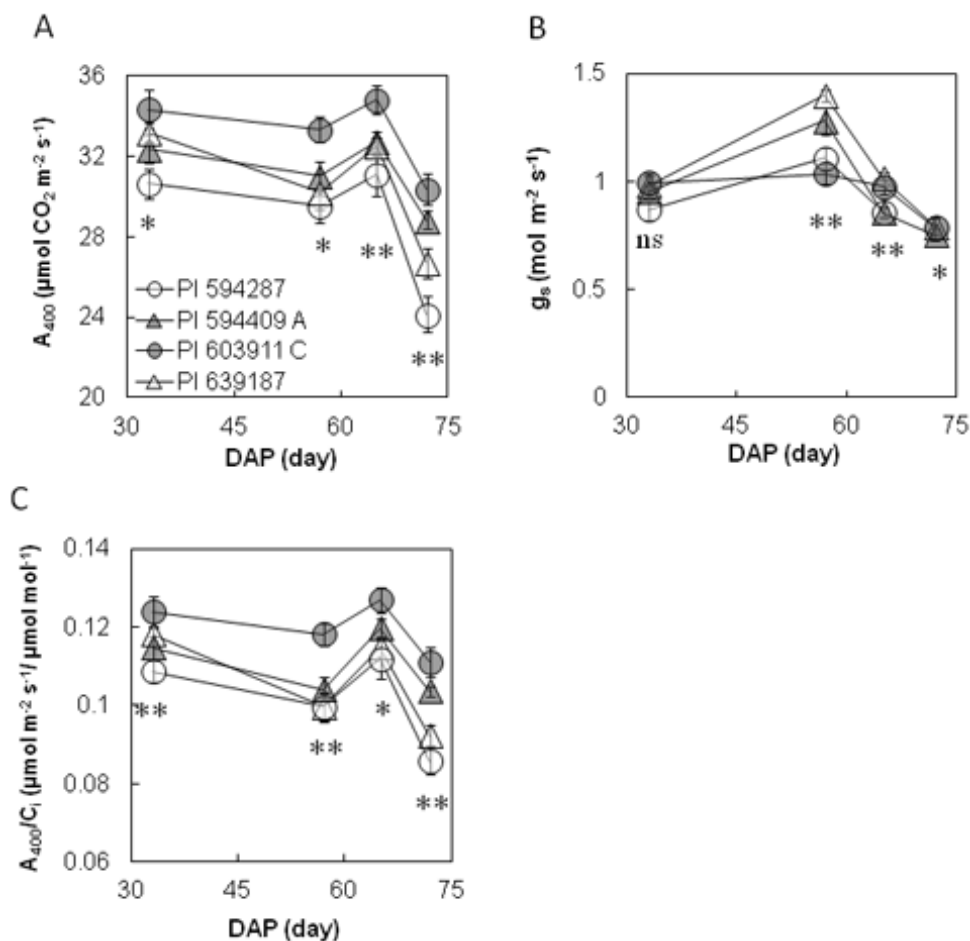


Fig. 2. CO_2 assimilation rate, stomatal conductance, and the CO_2 assimilation rate (A_{400}) to intercellular CO_2 concentration (C_i) ratio of four soybean genotypes. (A) A_{400} , (B) stomatal conductance, and (C) A_{400}/C_i at a CO_2 concentration of $400 \mu\text{mol mol}^{-1}$, all measured in the field from the upper-most fully expanded leaf at 33, 57, 65, and 72 d after planting (DAP) of PI 639187 (UA) (open triangle), PI 594287 (Tc) (open circle), PI 594409 A (Line no. 13) (gray triangle), and PI 603911 C (Line no. 14) (gray circle). Asterisks, * and **, indicates the significant difference among four soybean genotypes at $P < 0.05$ and 0.01 , respectively.

(the simple indicator of CO_2 fixation activity) in Line no. 14 was consistently higher than that of the others throughout all the measurements (Fig. 2C). There was a significant variation of A_{400} , stomatal conductance, and A_{400}/C_i among four genotypes throughout all the measurements except that of stomatal conductance at 33 DAP ($P < 0.05$). The $A-C_i$ curve analysis showed that Line no. 14 exhibited the highest A under all the CO_2 conditions except for 59 DAP (Fig. 3). The $V_{c_{\max}}$ and J_{\max} values of Line no. 14 were 129.1 and $232.0 \mu\text{mol m}^{-2} \text{s}^{-1}$, respectively, and were highest among four genotypes at 67 DAP ($P < 0.01$; Fig. 4). The changing pattern of $V_{c_{\max}}$ and J_{\max} in Lines no. 13 and 14 and UA was similar, while that of Tc was different.

Leaf Anatomy

In Exp. 2, the leaf structure was analyzed in the same leaf from which the $A-C_i$ curves were obtained on 67 and 71 DAP (Fig. 5; Supplemental Fig. S1). Leaf thickness varied from $164.4 \mu\text{m}$ in Line no. 13 to $248.0 \mu\text{m}$ in Line no. 14 at 67 DAP (Table 3). It ranged from $188.7 \mu\text{m}$ in UA to 235.9

μm in Line no. 14 at 71 DAP. Leaf thickness of Line no. 14 was significantly higher than that of the others at 67 DAP ($P < 0.05$). The palisade layer thickness varied from $95.5 \mu\text{m}$ in Line no. 13 to $150.5 \mu\text{m}$ in Line no. 14 at 67 DAP. It ranged from $101.8 \mu\text{m}$ in UA to $141.5 \mu\text{m}$ in Line no. 14 at 71 DAP. The palisade layer thickness of Line no. 14 was significantly higher than that of Line no. 13 and UA at 67 DAP and UA at 71 DAP ($P < 0.05$). The ratio of the palisade layer thickness to the leaf thickness (palisade/leaf ratio) ranged from 0.53 in UA to 0.62 in Tc at 67 DAP and 0.54 in UA to 0.6 in Line no. 14 at 71 DAP. There was a significant difference of palisade/leaf ratio between Line no. 14 and UA at 67 DAP ($P < 0.05$). The palisade/leaf ratio of all the genotypes was stable across the two measurements.

Quantification of Total Soluble Protein, Chlorophyll, Rubisco, and Nitrogen

In Exp. 2, the total soluble protein, chlorophyll, Rubisco, and N contents were determined with the same leaf from which leaf gas exchange was measured. The levels of these

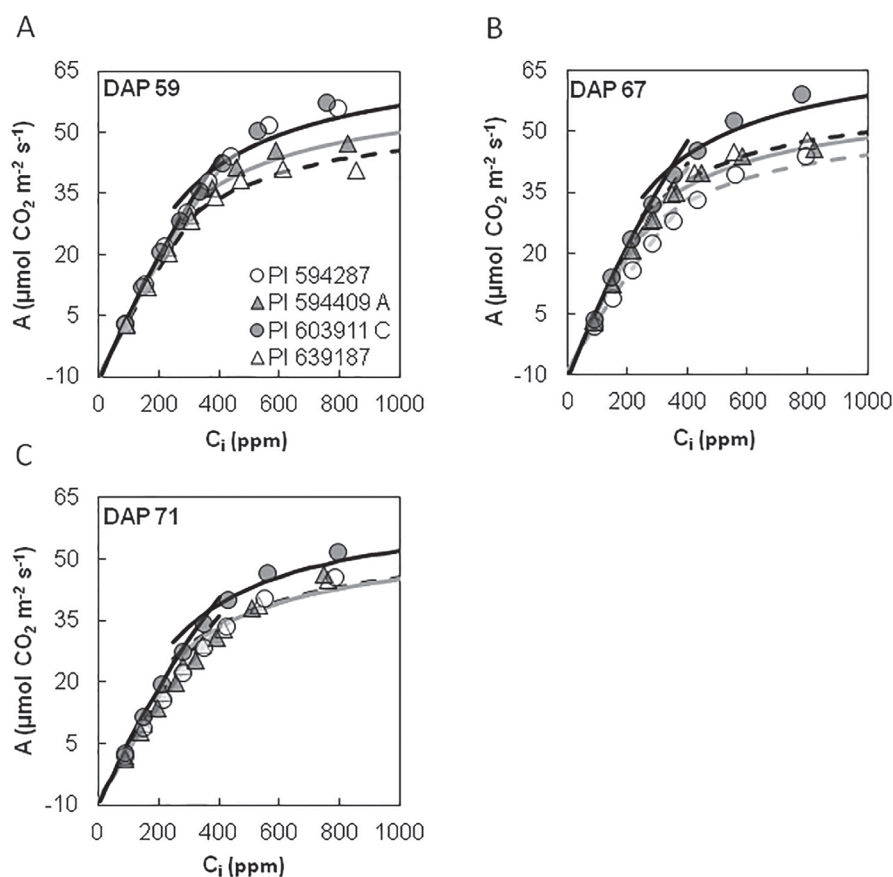


Fig. 3. Response curve of CO₂ assimilation rate (*A*) to intercellular CO₂ concentration (*C_i*) in four soybean genotypes. *A*–*C_i* curves were obtained from the upper-most fully expanded leaf at (A) 59 d after planting (DAP), (B) 67 DAP, and (C) 71 DAP of PI 639187 (UA) (open triangle), PI 594287 (Tc) (open circle), PI 594409 A (Line no. 13) (gray triangle), and PI 603911 C (Line no. 14) (gray circle).

components drastically increased around R5, but it was relatively stable during the other stages in all four genotypes (Fig. 6). The total soluble protein content ranged from 4.56 g m⁻² in Line no. 13 to 6.19 g m⁻² in UA before R5 and from 8.46 g m⁻² in UA to 11.0 g m⁻² in Tc after R5 (Fig. 6A). The chlorophyll content ranged from 268 mg m⁻² in Line no. 13 to 392 mg m⁻² in Tc before R5 and from 458 mg m⁻² in Line no. 14 to 610 mg m⁻² in Line no. 13 after R5 (Fig. 6B). The Rubisco content ranged from 1.51 g m⁻² in Tc to 2.41 g m⁻² in Line no. 14 before R5 and from 3.88 g m⁻² in UA and 5.31 g m⁻² in Line no. 14 after R5 (Fig. 6C). The N content ranged from 1.60 g m⁻² in Line no. 13 to 2.05 g m⁻² in UA before R5 and from 2.38 g m⁻² in Line no. 13 to 3.13 g m⁻² in Line no. 14 after R5 (Fig. 6D). There was no clear trend in the content of each component among the four genotypes before R5. After R5, the chlorophyll content in Line no. 13 and the Rubisco and N content in Line no. 14 tended to be higher than the equivalent values in other genotypes.

DISCUSSION

Several studies have reported on the natural variation in leaf photosynthetic capacity in soybean (Dornhoff and Shibles, 1970; Ojima, 1972; Buttery et al., 1981; Morrison

et al., 1999; Jin et al., 2010). The linear increase of the soybean photosynthetic rate was reported against year of release, and newer cultivars had up to 23% greater photosynthetic rate than older cultivars (Koester et al., 2016). In this study, the photosynthetic rate varied more than 50% among 34 soybean genotypes under controlled conditions (Fig. 1). These results suggest that there is a considerable variation of the leaf photosynthetic capacity not only among historical soybean cultivars but also among the Asian local genotypes. This variation can be exploited for the further genetic improvement of leaf photosynthetic capacity in soybean. In the present study, high photosynthetic capacity was attributed to the greater CO₂ fixation activity partly sustained by the higher Rubisco content and thicker leaf structure. On the other hand, the historical improvement of the photosynthetic capacity mostly depends on the greater stomatal conductance (Koester et al., 2016). Hence, the present study demonstrates the different path to the improvement of the leaf photosynthesis than the one occurred during the historical improvement.

The relative levels of leaf photosynthetic capacity among Line no. 14, Tc, and UA were conserved across Exp. 1 and 2. Line no. 14 consistently showed greater photosynthetic capacity than the others throughout the

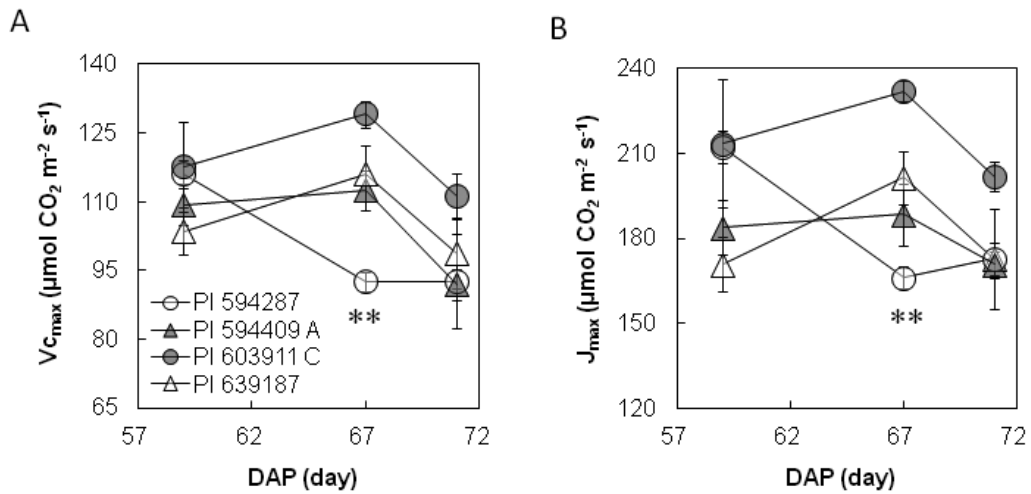


Fig. 4. Maximum carboxylation rate ($V_{c_{max}}$) and electron transport rate (J_{max}) of four soybean genotypes. DAP, days after planting. (A) $V_{c_{max}}$ and (B) J_{max} , estimated from the $A-C_i$ curves in Fig. 3 using the biochemical model described by Farquhar et al. (1980) for PI 639187 (UA) (open triangle), PI 594287 (Tc) (open circle), PI 594409 A (Line no. 13) (gray triangle), and PI 603911 C (Line no. 14) (gray circle). Double asterisks (**) indicates the significant difference among four soybean genotypes at $P < 0.01$.

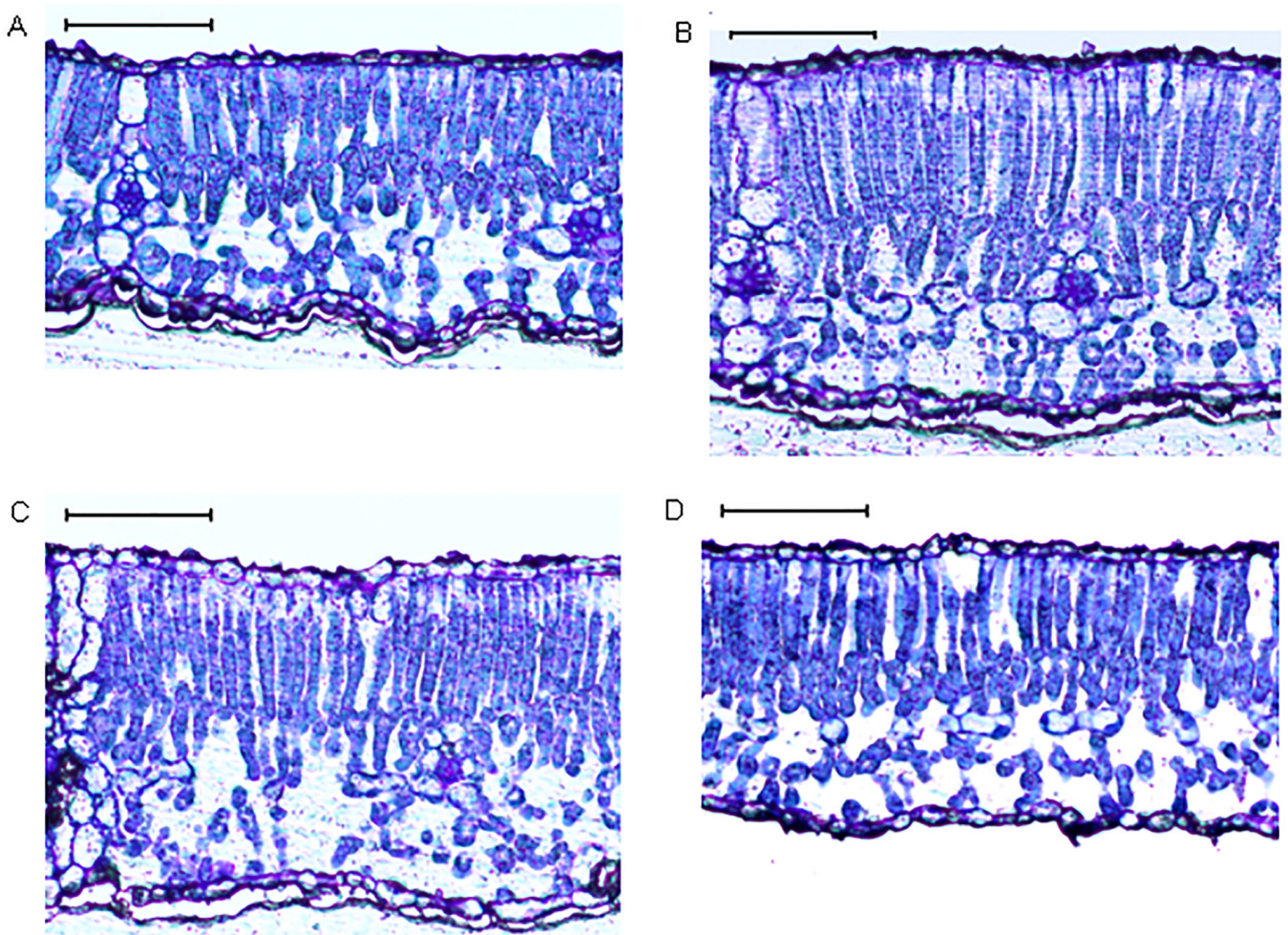


Fig. 5. Microscopic images of the leaf anatomical structure of four soybean genotypes. Microscopic images of the leaf anatomical structure were obtained in the same leaf at which $A-C_i$ measurements were conducted on 71 with (A) PI 594409 A (Line no. 13), (B) PI 603911 C (Line no. 14), (C) PI 594287 (Tc) and (D) PI 639187 (UA). Scale bars in each figure are equal to 100 μm .

Table 3. The leaf thickness, the palisade layer thickness, and the ratio of the palisade layer thickness to the leaf thickness. The leaf anatomical structure was analyzed in resin sections to measure the leaf thickness, the palisade thickness and the ratio of the palisade thickness to the leaf thickness in PI 639187 (UA), PI 594287 (Tc), PI 594409 A (Line no. 13) and PI 603911 C (Line no. 14). The value of the leaf thickness, the palisade thickness, and the ratio of the palisade thickness to the leaf thickness are the means for $n = 3$.

	67 d after planting				71 d after planting			
	UA	Tc	Line no. 13	Line no. 14	UA	Tc	Line no. 13	Line no. 14
Leaf thickness, μm	194.5bc†	204.6b	164.4c	248.0a	188.7a	226.7a	197.5a	235.9a
Palisade layer thickness, μm	102.7bc	125.9ab	95.5c	150.5a	101.8b	132.1ab	116.5ab	141.5a
Palisade/leaf	0.53b	0.62a	0.58ab	0.61a	0.54a	0.58a	0.59a	0.60a

† Different letters following each value mean they are significantly different.

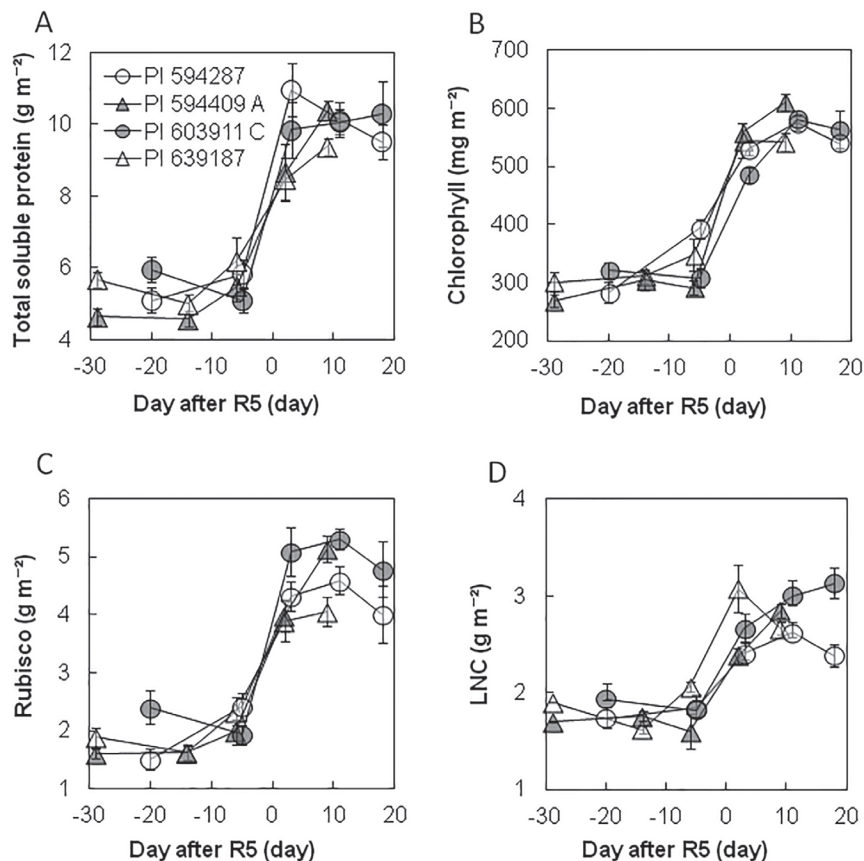


Fig. 6. Total soluble protein, chlorophyll, Rubisco, and nitrogen (LNC) content. The content of (A) total soluble protein, (B) chlorophyll, (C) Rubisco, and (D) nitrogen, measured at the same leaf position as the measurement of leaf gas exchange, on 33, 57, 65, and 72 d after planting (DAP) from PI 639187 (UA) (open triangle), PI 594287 (Tc) (open circle), PI 594409 A (Line no. 13) (gray triangle), and PI 603911 C (Line no. 14) (gray circle). Vertical bars indicate the standard error (SE) of seven to ten replicates for each genotype.

flowering and seed filling stages in the field (Fig. 2A). This confirms that Line no. 14 is useful candidate for identifying the mechanism underlying high photosynthetic capacity in soybean. The A_{380} values of Line no. 13 were the highest among all the soybean genotypes in Exp. 1 because of that strain's high stomatal conductance. On the other hand, the A_{400} values of Line no. 13 were similar to those of UA, the reference cultivar in Exp. 2. This was because there was no clear difference in stomatal conductance among the four genotypes in Exp. 2, and Line no. 13 had no advantage that would allow it to achieve a high photosynthetic rate. Differences in the environmental

conditions or in the growth stage of the plants between Exp. 1 and 2 might be the cause of this inconsistency.

Leaf photosynthetic capacity is determined by both the CO₂ supply from atmosphere to the chloroplast and also by CO₂ fixation at the chloroplast (Farquhar et al., 1980). It is well known that stomatal conductance strongly affects leaf photosynthetic capacity (Farquhar and Sharkey 1982). Ohsumi et al. (2007) reported that stomatal conductance was one of the major factors determining the natural variation in leaf photosynthetic capacity in rice. A correlation between leaf photosynthetic rate and stomatal conductance was also observed among soybean genotypes under field

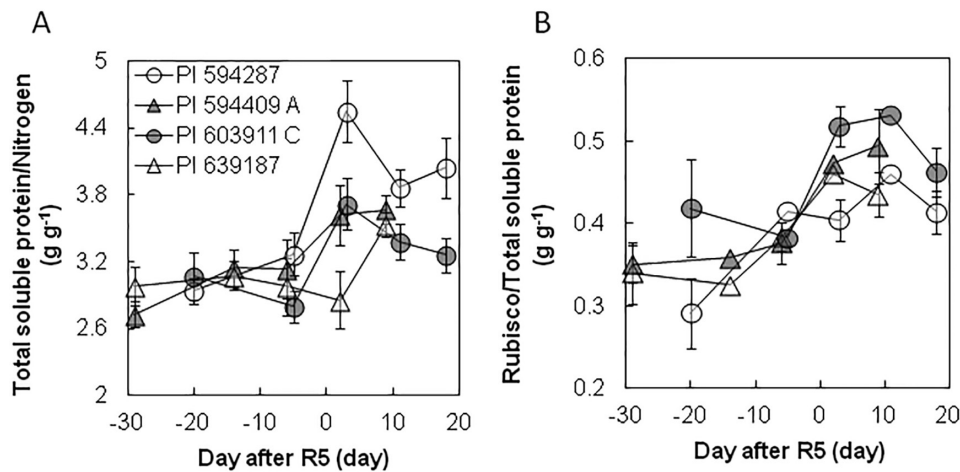


Fig. 7. Ratio of total soluble protein to N and Rubisco to total soluble protein. The ratio of total soluble protein to N and the ratio of Rubisco to total soluble protein were calculated at 33, 57, 65, and 72 d after planting (DAP) in PI 639187 (UA) (open triangle), PI 594287 (Tc) (open circle), PI 594409 A (Line no. 13) (gray triangle), and PI 603911 C (Line no. 14) (gray circle). Vertical bars indicate the standard error (SE) of seven to 10 replicates for each genotype.

conditions (Tanaka et al., 2008). This correlation, however, was not observed among the 34 soybean genotypes in Exp. 1 (data not shown). There was no clear relationship between A_{400} and stomatal conductance in Exp. 2 (Fig. 2A–B). These results suggest that stomatal conductance did not regulate the variation in the leaf photosynthetic capacity among the soybean genotypes used in the present study.

In Exp. 2, the stomatal conductance of Line no. 14 was similar to that of UA, while the A_{400}/C_i , $V_{c_{max}}$, and J_{max} values of Line no. 14 were consistently the highest among the four genotypes throughout the reproductive stage (Fig. 2B–C, 4). These results showed that greater CO_2 fixation activity contributed to the high leaf photosynthetic rate of Line no. 14. Leaf N content is one of the most important traits determining leaf photosynthetic capacity because a large portion of leaf N is allocated to the photosynthetic components, especially to Rubisco (Hikosaka, 2010). The amount and kinetics of Rubisco limit CO_2 fixation activity. It has been reported that the Rubisco content and its activity determined the changes in leaf photosynthetic capacity in the course of senescence under field conditions in soybean (Jiang et al., 1993). In the present study, the N and Rubisco content in Line no. 14 tended to be higher than in other genotypes (Fig. 6C–D). The leaves of Line no. 14 was also thicker than the leaves of the other genotypes (Table 3). It has been reported that leaf photosynthetic capacity is correlated with leaf thickness and nitrogen content in soybean (Ojima, 1972). These results imply that a thicker leaf can accumulate a large amount of nitrogen and photosynthetic apparatus, and have an advantage in achieving high photosynthetic capacity.

Tc showed the similar value of $V_{c_{max}}$ and J_{max} to Line no. 14 at 59 DAP (Fig. 4). Tc and Line no. 14 reached R5 at 54 DAP (Table 2). These results indicated that Tc had the potential to archive high CO_2 fixation activity parallel

with that of Line no. 14 at R5. Line no. 14 maintained higher total soluble protein, Rubisco, and N content than Tc after R5 (Fig. 6A, 6C–D). It might be, therefore, related to the difference of the changing pattern of CO_2 fixation activity between these genotypes.

The ratio of total soluble protein to N in Line no. 14 was similar to or lower than that seen in the other genotypes (Fig. 7A). On the other hand, the ratio of Rubisco to total soluble protein in Line no. 14 was higher than in the other genotypes (Fig. 7B). This shows that the large amount of Rubisco in Line no. 14 can be attributed to the greater distribution of total soluble protein. Kawasaki et al. (2014) reported that there was considerable variation in the ratio of Rubisco to N in soybean under field conditions. Thus, protein distribution in the leaf can also be a target to select soybean genotypes with high photosynthetic capacity.

The Rubisco content of Tc was similar to that of UA and Line no. 13, while the leaf photosynthetic capacity and the CO_2 fixation activity of Tc was lower than that of the other genotypes in Exp. 2 (Fig. 2A, 2C, 4, 6C). This suggests that factors other than Rubisco content, such as Rubisco kinetics and its activation state, can also affect variation in leaf photosynthetic capacity. In addition, $V_{c_{max}}$ and J_{max} were estimated based on C_i in this study. It is assumed that mesophyll conductance is infinite in all the genotypes. Evidence has accumulated, however, showing that mesophyll conductance is highly variable and affects leaf photosynthetic rate (Flexas et al., 2008). Thus, the inconsistency between Rubisco content and CO_2 fixation activity found in Exp. 2 might also reflect variation in mesophyll conductance among these genotypes. In a future study, the effect of Rubisco activity, its activation state, and mesophyll conductance on leaf photosynthetic capacity in soybean have to be elucidated.

In conclusion, considerable variation in leaf photosynthetic capacity was observed among 34 soybean genotypes, and a high photosynthetic genotype, PI 603911 C (Line no. 14), was identified. Carbon dioxide fixation, rather than CO₂ supply, was the major factor responsible for the high photosynthetic capacity of this genotype. Line no. 14 accumulated a large amount of Rubisco because of the greater allocation of total soluble protein to Rubisco. These results demonstrate the considerable potential for genetic enhancement of leaf photosynthetic capacity in soybean.

Supplemental Information Available

Supplemental information is available with the online version of this manuscript.

Acknowledgments

A part of this study was supported by a grant from the Ministry of Agriculture, Forestry, and Fisheries of Japan (Genomics-based Technology for Agricultural Improvement, SFC1002), the Realizing Increased Photosynthetic Efficiency (RIPE) project, and the John Mung Program of Kyoto University. We are grateful to Dr. Randall Nelson of the University of Illinois, Urbana-Champaign, and Jeffery Ray of USDA-ARS, Mississippi, for providing plant materials; Dr. Sho Ohno of Kyoto University for assistance in analyzing leaf anatomical structure; and Dr. Yoshitaka Takano of Kyoto University for assistance with the protein analysis.

References

- Adachi, S., T. Nakae, M. Uchida, K. Soda, T. Takai, T. Oi, et al. 2013. The mesophyll anatomy enhancing CO₂ diffusion is a key trait for improving rice photosynthesis. *J. Exp. Bot.* 64:1061–1072. doi:10.1093/jxb/ers382
- Ainsworth, E.A., and S.P. Long. 2005. What have we learned from 15 years of free-air CO₂ enrichment (FACE)? A meta-analytic review of the responses of photosynthesis, canopy properties and plant production to rising CO₂. *New Phytol.* 165:351–372. doi:10.1111/j.1469-8137.2004.01224.x
- Bernacchi, C.J., E.L. Singaas, C. Pimentel, A.R. Portis, Jr., and S.P. Long. 2001. Improved temperature response functions for models of Rubisco-limited photosynthesis. *Plant Cell Environ.* 24:253–259. doi:10.1111/j.1365-3040.2001.00668.x
- Bradford, M.M. 1976. A Rapid and sensitive method for the quantitation of microgram quantities of protein utilizing the principle of protein-dye binding. *Anal. Biochem.* 72:248–254. doi:10.1016/0003-2697(76)90527-3
- Buttery, B.R., R.I. Buzzell, and W.I. Findlay. 1981. Relationships among photosynthetic rate, bean yield and other characters in field-grown cultivars of soybean. *Can. J. Plant Sci.* 61:190–197. doi:10.4141/cjps81-029
- Cohen, J.E. 2003. Human population: The next half century. *Science* 302:1172–1175. doi:10.1126/science.1088665
- Dornhoff, G.M., and R.M. Shibles. 1970. Varietal differences in net photosynthesis of soybean leaves. *Crop Sci.* 10:42–45. doi:10.2135/cropsci1970.0011183X001000010016x
- Evans, J.R. 1989. Photosynthesis and nitrogen relationships in leaves of C₃ plants. *Oecologia* 78:9–19. doi:10.1007/BF00377192
- Farquhar, G.D., and T.D. Sharkey. 1982. Stomatal conductance and photosynthesis. *Plant Physiol.* 33:317–345. doi:10.1146/annurev.pp.33.060182.001533
- Farquhar, G.D., S. von Cammerer, and J.A. Berry. 1980. A biochemical model of photosynthetic CO₂ assimilation in leaves of C₃ species. *Planta* 149:78–90. doi:10.1007/BF00386231
- Flexas, J., M. Ribas-Carbo, A. Diaz-Espejo, J. Galmes, and H. Medrano. 2008. Mesophyll conductance to CO₂: Current knowledge and future prospects. *Plant Cell Environ.* 31:602–621. doi:10.1111/j.1365-3040.2007.01757.x
- Flood, P.J., J. Harbinson, and M.G.M. Aarts. 2011. Natural genetic variation in plant Photosynthesis. *Trends Plant Sci.* 16:327–335. doi:10.1016/j.tplants.2011.02.005
- Franks, P.J., and D.J. Beerling. 2009. Maximum leaf conductance driven by CO₂ effects on stomatal size and density over geologic time. *Proc. Natl. Acad. Sci. USA* 106:10343–10347. doi:10.1073/pnas.0904209106
- Hikosaka, K. 2004. Interspecific difference in the photosynthesis-nitrogen relationship: Patterns, physiological causes, and ecological importance. *J. Plant Res.* 117:481–494. doi:10.1007/s10265-004-0174-2
- Hikosaka, K. 2010. Mechanisms underlying interspecific variation in photosynthetic capacity across wild plant species. *Plant Biotechnol.* 27:223–229. doi:10.5511/plantbiotechnology.27.223
- Jiang, C.Z., S.R. Rodermel, and R.M. Shibles. 1993. Photosynthesis, Rubisco activity and amount, and their regulation by transcription in senescing soybean leaves. *Plant Physiol.* 101:105–112.
- Jin, J., X. Liu, G. Wang, L. Mi, Z. Shen, X. Chen, et al. 2010. Agronomic and physiological contributions to the yield improvement of soybean cultivars released from 1950 to 2006 in Northeast China. *Field Crops Res.* 115:116–123. doi:10.1016/j.fcr.2009.10.016
- Kanemura, T., K. Homma, A. Ohsumi, T. Shiraiwa, and T. Horie. 2007. Evaluation of genotypic variation in leaf photosynthetic rate and its associated factors by using rice diversity research set of germplasm. *Photosynth. Res.* 94:23–30. doi:10.1007/s1120-007-9208-7
- Kawasaki, Y., Y. Tanaka, K. Katsura, L.C. Purcell, and T. Shiraiwa. 2016. Yield and dry matter productivity of Japanese and US soybean cultivars. *Plant Production Science.* 19:257–266. doi:10.1080/1343943X.2015.1133235
- Kawasaki, Y., Y. Tanaka, K. Katsura, and T. Shiraiwa. 2014. Dry matter production and nitrogen utilization of high yielding soybean cultivars. Presented at: Grand challenges: Great solutions. ASA, CSSA, and SSSA Annual Meetings, Long Beach, CA. 2–5 Nov. 2014. Poster 394-17.
- Koester, R.P., B.M. Nohli, B.W. Diers, and E.A. Ainsworth. 2016. Has photosynthetic capacity increased with 80 years of soybean breeding? An examination of historical soybean cultivars. *Plant Cell Environ.* 39:1058–1067. doi:10.1111/pce.12675
- Koester, R.P., J.A. Skoneczka, T.R. Cary, B.W. Diers, and E.A. Ainsworth. 2014. Historical gains in soybean (*Glycine max* Merr.) seed yield are driven by linear increases in light interception, energy conversion, and partitioning efficiencies. *J. Exp. Bot.* 65:3311–3321. doi:10.1093/jxb/eru187
- Lawson, T., and M.R. Blatt. 2014. Stomatal size, speed, and responsiveness impact on photosynthesis and water use efficiency. *Plant Physiol.* 164:1556–1570. doi:10.1104/pp.114.237107
- Long, S.P., X.G. Zhu, S.L. Naidu, and D.R. Ort. 2006. Can improvement in photosynthesis increase crop yields? *Plant Cell Environ.* 29:315–330. doi:10.1111/j.1365-3040.2005.01493.x
- Makino, A., T. Mae, and K. Ohira. 1986. Colorimetric measurement of protein stained with Coomassie Brilliant Blue R on

- sodium dodecyl sulfate–polyacrylamide gel electrophoresis by eluting with formamide. *Agric. Biol. Chem.* 50:1911–1912.
- McMurtrie, R.E., and Y.P. Wang. 1993. Mathematical models of the photosynthetic response of tree stands to rising CO₂ concentrations and temperatures. *Plant Cell Environ.* 16:1–13. doi:10.1111/j.1365-3040.1993.tb00839.x
- Mitchell, R.A.C., C.R. Black, S. Burkart, J.I. Burke, A. Donnelly, L. de Temmerman, et al. 1999. Photosynthetic responses in spring wheat grown under elevated CO₂ concentrations and stress conditions in the European, multiple-site experiment ‘SPACE-wheat’. *Eur. J. Agron.* 10:205–214. doi:10.1016/S1161-0301(99)00010-6
- Morrison, M.J., H.D. Voldeng, and E.R. Cober. 1999. Physiological changes from 58 years of genetic improvement of short-season soybean cultivars in Canada. *Agron. J.* 91:685–689. doi:10.2134/agronj1999.914685x
- Ohsumi, A., A. Hamasaki, H. Nakagawa, H. Yoshida, T. Shiraiwa, and T. Horie. 2007. A model explaining genotypic and ontogenetic variation of leaf photosynthetic rate in rice (*Oryza sativa*) based on leaf nitrogen content and stomatal conductance. *Ann. Bot. (Lond.)* 99:265–273. doi:10.1093/aob/mcl253
- Ojima, M. 1972. Improvement of leaf photosynthesis in soybean varieties. (In Japanese with English abstract.) *Bull. Natl. Inst. Agric. Sci. Ser. D.* 23:97–154.
- Porra, R.J., W.A. Thompson, and P.E. Kriedemann. 1989. Determination of accurate extinction coefficients and simultaneous equations for assaying chlorophylls a and b extracted with four different solvents: Verification of the concentration of chlorophyll standards by atomic absorption spectroscopy. *Biochim. Biophys. Acta, Bioenerg.* 975:384–394. doi:10.1016/S0005-2728(89)80347-0
- Raines, C.A. 2011. Increasing photosynthetic carbon assimilation in C₃ plants to improve crop yield: Current and future strategies. *Plant Physiol.* 155:36–42. doi:10.1104/pp.110.168559
- Ray, J.D., A.P. Dhanapal, S.K. Singh, V. Hoyos-Villegas, J.R. Smith, L.C. Purcell, et al. 2015. Genome-wide association study of ureide concentration in diverse maturity group IV soybean [*Glycine max* (L.) Merr.] accessions. G3: Genes, Genomes, Genet. 5:2391–2403. doi:10.1534/g3.115.021774
- R Development Core Team. 2010. R: A language and environment for statistical computing. R Foundation for Stat. Comput., Vienna, Austria.
- Schneider, C.A., W.S. Rasband, K.W. Eliceiri. 2012. NIH Image to ImageJ: 25 years of image analysis. *Nature Methods* 9, 671–675. doi:10.1038/nmeth.2089
- Sinclair, T.R., and T. Horie. 1989. Leaf nitrogen, photosynthesis, and crop radiation use efficiency: A review. *Crop Sci.* 29:90–98.
- Takai, T., S. Adachi, F. Taguchi-Shiobara, Y. Sanoh-Arai, N. Iwasawa, S. Yoshinaga, et al. 2013. A natural variant of *NAL1*, selected in high-yield rice breeding programs, pleiotropically increases photosynthesis rate. *Sci. Rep.* 3:2149. doi:10.1038/srep02149
- Tanaka Y., Y. Fukuda, K. Nakashima, and T. Shiraiwa. 2013. High-throughput phenotyping of the leaf transpiration at the primary leaf in soybean [*Glycine max* (L.) Merr.]. Poster presented at: Water, Food, Energy & Innovation for a Sustainable World. ASA, CSSA, and SSSA Annual Meetings, Tampa, Florida. 3–6 Nov. Poster 370–13.
- Tanaka, Y., K. Fujii, and T. Shiraiwa. 2010. Variability of leaf morphology and stomatal conductance in soybean [*Glycine max* (L.) Merr.] cultivars. *Crop Sci.* 50:2525–2532. doi:10.2135/cropsci2010.02.0058
- Tanaka, Y., T. Shiraiwa, A. Nakajima, J. Sato, and T. Nakazaki. 2008. Leaf gas exchange activity in soybean as related to leaf traits and stem growth habit. *Crop Sci.* 48:1925–1932. doi:10.2135/cropsci2007.12.0707
- USDA. 2012. Soybeans and oil crops: Overview. USDA Economic Research Service. <http://www.ers.usda.gov/topics/crops/soybeans-oil-crops.aspx> (accessed 24 Feb. 2016).
- Zhu, X.G., S.P. Long, and D.R. Ort. 2010. Improving photosynthetic efficiency for greater yield. *Annu. Rev. Plant Biol.* 61:235–261. doi:10.1146/annurev-arplant-042809-112206